

# Conformational Characterization of Glycine Residues Incorporated into Some Homopolypeptides by Solid-State $^{13}\text{C}$ NMR Spectroscopy

Shinji Ando,<sup>†</sup> Takeshi Yamanobe,<sup>†</sup> Isao Ando,<sup>\*†</sup> Akira Shoji,<sup>†</sup> Takuo Ozaki,<sup>†</sup> Ryoko Tabeta,<sup>§</sup> and Hazime Saitô<sup>§</sup>

Contribution from the Department of Polymer Chemistry, Tokyo Institute of Technology, Ookayama, Meguro-ku, Tokyo, Japan 152, the Department of Industrial Chemistry, College of Technology, Gunma University, Tenjin-cho, Kiryu-shi, Gunma, Japan 376, and the Biophysics Division, National Cancer Center Research Institute, Tsukiji, Chuo-ku, Tokyo, Japan 104. Received April 29, 1985

**Abstract:**  $^{13}\text{C}$  NMR spectra of a variety of polypeptides containing  $^{13}\text{C}$ -enriched [ $1\text{-}^{13}\text{C}$ ]glycine [(Gly\*)] residue as a minor component (<8%) in the solid state were recorded, in order to obtain the  $^{13}\text{C}$  chemical shifts of isotropic averaging and the principal values of chemical shift tensors ( $\sigma_{11}$ ,  $\sigma_{22}$ , and  $\sigma_{33}$ ) of glycine carbonyl carbon (Gly CO), taking antiparallel  $\beta$ -sheet,  $3_1$ -helix,  $\alpha$ -helix, and  $\omega$ -helix forms. The latter two conformations are achieved only when Gly residues are incorporated into the homopolypeptides, taking the respective conformations. It was found that the isotropic Gly CO chemical shifts are significantly displaced depending on conformational change. We also found that the magnitudes of displacements of chemical shifts upon conformational changes are larger for  $\sigma_{22}$  and  $\sigma_{33}$  than the isotropic chemical shift values, while  $\sigma_{11}$  is almost unchanged upon any conformational changes.

It has been demonstrated that  $^{13}\text{C}$  NMR chemical shifts of a number of polypeptides and proteins in the solid state as determined by the cross polarization-magic angle spinning (CP-MAS) method are significantly displaced depending on their particular conformations such as  $\alpha$ -helix,  $\beta$ -sheet,  $3_1$ -helix, and  $\omega$ -helix.<sup>1-9</sup> In particular, the  $^{13}\text{C}$  chemical shifts of individual amino acid residues of peptides and proteins are not strongly influenced by a specific amino acid sequence<sup>4-6</sup> but by the local conformation of the residues under consideration, as defined by the torsional angles ( $\phi$  and  $\psi$ ) of the skeletal bonds. This view was supported by our theoretical calculation of the contour map of the  $^{13}\text{C}$  chemical shift utilizing the finite perturbation (FPT-INDO) theory<sup>10</sup> and the sum-over-state tight-binding MO theory.<sup>11</sup> This approach permits one to use the conformation-dependent  $^{13}\text{C}$  chemical shift as an intrinsic probe to elucidate the conformational feature in the solid states as viewed from the individual amino acid residues under consideration. Thus, it is feasible to carry out conformational characterization of a number of polypeptides, if the  $^{13}\text{C}$  chemical shifts of suitable reference polypeptides are available.

On the other hand, it is expected that the principal values of  $^{13}\text{C}$  chemical shift tensors ( $\sigma_{11}$ ,  $\sigma_{22}$ , and  $\sigma_{33}$ ) are more valuable as parameters for chemical informations to be related with electronic structure than the isotropically averaged value ( $\sigma_{\text{iso}} = 1/3(\sigma_{11} + \sigma_{22} + \sigma_{33})$ ) which is determined by MAS. Nevertheless, very few data are available for the  $^{13}\text{C}$  chemical shift tensor of a carbon of a peptide bond, except for that of collagen labeled with [ $1\text{-}^{13}\text{C}$ ]glycine,<sup>12</sup> poly(glycine),<sup>12</sup> and [ $1\text{-}^{13}\text{C}$ ]glycyl-[ $^{15}\text{N}$ ]glycine.<sup>13</sup> This sort of values has been used to detect the presence or absence of molecular motions as viewed from the breadth ( $\sigma_{33} - \sigma_{11}$ ). No attempt, however, has been made to relate the principal values of tensors to conformational feature. As a continuation of our effort to relate the conformation-dependent isotropic chemical shifts of polypeptides to their particular conformation in the solid state, it is natural to expect that the individual components of the tensor also vary with molecular conformations. Especially, it is very important to know how these components are varied with the torsional angles as well as the manner of hydrogen bondings for the understanding of the conformation-dependent  $^{13}\text{C}$  chemical shifts.

In this paper, we attempt to analyze and argue isotropic  $^{13}\text{C}$  chemical shifts and individual components of  $^{13}\text{C}$  chemical shift

tensors of the glycine residue (Gly) of polypeptides taking various conformations such as  $\beta$ -sheet,  $3_1$ -helix,  $\alpha$ -helix, and  $\omega$ -helix forms. The conformations of the last two forms are achieved by incorporation of a small amount of [ $1\text{-}^{13}\text{C}$ ]Gly residue (<8%) into polypeptides taking respective conformations. For this purpose,  $^{13}\text{C}$ -enriched [ $1\text{-}^{13}\text{C}$ ]glycine residues are incorporated into polypeptides such as poly(glycine) [(Gly)<sub>n</sub>], poly(L-alanine) [(Ala)<sub>n</sub>], poly(L-leucine) [(Leu)<sub>n</sub>], poly( $\gamma$ -benzyl L-glutamate) [(Glu(OBzl))<sub>n</sub>], poly( $\beta$ -benzyl L-aspartate) [(Asp(OBzl))<sub>n</sub>], and poly(L-valine) [(Val)<sub>n</sub>].

## Experimental Section

**Materials.** Poly([ $1\text{-}^{13}\text{C}$ ]glycine). Poly([ $1\text{-}^{13}\text{C}$ ]glycine),  $^{13}\text{C}$  purity of which was 30 atom %, was prepared by heterogeneous polymerization of [ $1\text{-}^{13}\text{C}$ ]glycine *N*-carboxyanhydride (NCA) in acetonitrile by using *n*-butylamine as the initiator, which was synthesized from a mixture of [ $1\text{-}^{13}\text{C}$ ]glycine (Merck, Inc., Lot No. 1442G, isotope purity 90 atom %) and glycine (Nihon-Rika). The mole ratio of NCA to initiator (A/I) was chosen as 100 and 5. The polymer of A/I = 100 took antiparallel  $\beta$ -sheet [(Gly)<sub>n</sub>I] form. Conformation of this sample was converted to  $3_1$ -helix [(Gly)<sub>n</sub>II] either by the procedure of precipitation from aqueous lithium bromide solution<sup>14</sup> or by casting from formic acid solution saturated with calcium chloride.<sup>15</sup> The averaged degree of polymerization for the

(1) Taki, T.; Yamashita, S.; Satoh, M.; Shibata, A.; Yamashita, T.; Tabeta, R.; Saitô, H. *Chem. Lett.* **1981**, 1803.

(2) Saitô, H.; Tabeta, R.; Shoji, A.; Ozaki, T.; Ando, I. *Macromolecules* **1983**, *16*, 1050.

(3) Saitô, H.; Tabeta, R.; Ando, I.; Ozaki, T.; Shoji, A. *Chem. Lett.* **1983**, 1437.

(4) Saitô, H.; Tabeta, R.; Asakura, T.; Iwanaga, Y.; Shoji, A.; Ozaki, T.; Ando, I. *Macromolecules* **1984**, *17*, 1405.

(5) Shoji, A.; Ozaki, T.; Saitô, H.; Tabeta, R.; Ando, I. *Macromolecules*, **1984**, *17*, 1472.

(6) Saitô, H.; Tabeta, R.; Shoji, A.; Ozaki, T.; Ando, I.; Miyata, T. *Biopolymers* **1984**, *23*, 2279.

(7) Kricheldorf, H. R.; Mutter, M.; Mazer, F.; Müller, D.; Forster, D. *Biopolymers* **1983**, *22*, 1357.

(8) Kricheldorf, H. R.; Müller, D. *Macromolecules* **1983**, *16*, 615.

(9) Kricheldorf, H. R.; Müller, D.; Ziegler, K. *Polymer Bull.* **1983**, *9*, 284.

(10) Ando, I.; Saitô, H.; Tabeta, R.; Shoji, A.; Ozaki, T. *Macromolecules* **1984**, *17*, 457.

(11) (a) Yamanobe, T.; Ando, I.; Saitô, H.; Tabeta, R.; Shoji, A.; Ozaki, T. *Bull. Chem. Soc. Jpn* **1985**, *58*, 23. (b) Yamanobe, T.; Ando, I.; Saitô, H.; Tabeta, R.; Shoji, A.; Ozaki, T. *Chem. Phys.* **1985**, *99*, 259.

(12) Jelinski, L. W.; Torchia, D. A. *J. Mol. Biol.* **1979**, *133*, 45.

(13) Stark, R. E.; Jelinski, L. W.; Ruben, D. J.; Torchia, D. A.; Griffin, R. G. *J. Magn. Reson.* **1983**, *55*, 266.

(14) Crick, F. H. C.; Rich, A. *Nature (London)* **1955**, *176*, 780.

<sup>†</sup> Tokyo Institute of Technology.

<sup>§</sup> Gunma University.

<sup>§</sup> National Cancer Center Research Institute.

**Table I.** Synthesis and Characterization of Poly([1-<sup>13</sup>C]glycine) and [1-<sup>13</sup>C]Glycine-Containing Polypeptides

sample <sup>a</sup>	Gly content, %	initiator	solvent	A/I ratio <sup>b</sup>	conformation <sup>c</sup>
(Gly*) <sub>n</sub> I	100	<i>n</i> -BuNH <sub>2</sub>	CH <sub>3</sub> CN	100	β-sheet
(Gly*) <sub>n</sub> II	100	<i>n</i> -BuNH <sub>2</sub>	CH <sub>3</sub> CN	100	3 <sub>1</sub> -helix
(Gly*) <sub>5</sub>	100	<i>n</i> -BuNH <sub>2</sub>	CH <sub>3</sub> CN	5	
(Ala,Gly*) <sub>n</sub>	5	<i>n</i> -BuNH <sub>2</sub>	CH <sub>3</sub> CN	100	α-helix
(Leu,Gly*) <sub>n</sub>	8	<i>n</i> -BuNH <sub>2</sub>	CH <sub>3</sub> CN	100	α-helix
(Glu(OBzl),Gly*) <sub>n</sub>	8	Et <sub>3</sub> N	ClCH <sub>2</sub> CH <sub>2</sub> Cl	100	α-helix
(Asp(OBzl),Gly*) <sub>n</sub>	8	Et <sub>3</sub> N	ClCH <sub>2</sub> CH <sub>2</sub> Cl	100	α-helix
(Asp(OBzl),Gly*) <sub>n</sub>	8	Et <sub>3</sub> N	ClCH <sub>2</sub> CH <sub>2</sub> Cl	100	ω-helix
(Val,Gly*) <sub>n</sub>	8	<i>n</i> -BuNH <sub>2</sub>	CH <sub>3</sub> CN	100	β-sheet

<sup>a</sup> Symbol \* indicates carbonyl carbon enriched by <sup>13</sup>C. <sup>b</sup> Theoretical number-averaged degree of polymerization. <sup>c</sup> Determined by the conformation-dependent <sup>13</sup>C NMR chemical shifts of host residues and partly by the characteristic bands in IR spectra.

sample of A/I = 5 was determined as ca. 5 from the <sup>1</sup>H NMR spectrum.

The conformational characterization of the host polypeptides was made on the basis of the conformation-dependent <sup>13</sup>C NMR chemical shifts<sup>1-6</sup> determined from the <sup>13</sup>C CP-MAS method and partly by the characteristic bands in the IR spectra. The samples prepared above for A/I = 100 gave almost identical IR and CP-MAS spectra to the respective reference data of homopolypeptides reported previously.<sup>1-6</sup> (According to this characterization, it is apparent that the molecular weights of the samples of A/I = 100 are sufficiently high enough to obtain desirable conformation.<sup>2</sup>)

**Copolypeptides.** A series of copolymers was prepared by polymerization of [1-<sup>13</sup>C]Gly NCA (90 atom %) with respective amino acid *N*-carboxyanhydrides, L-alanine, L-leucine, γ-benzyl L-glutamate, β-benzyl L-aspartate, and L-valine *N*-carboxyanhydrides. *n*-Butylamine and acetonitrile were used as the initiator and polymerization solvent, respectively, for poly(L-alanine,[1-<sup>13</sup>C]glycine) [(Ala,Gly\*)<sub>n</sub>], poly(L-leucine,[1-<sup>13</sup>C]glycine) [(Leu,Gly\*)<sub>n</sub>], and poly(L-valine,[1-<sup>13</sup>C]glycine) [(Val,Gly\*)<sub>n</sub>]. Dichloroethane and triethylamine were used as the initiator and polymerization solvent, respectively, for poly(γ-benzyl L-glutamate,[1-<sup>13</sup>C]glycine) [(Glu(OBzl),Gly\*)<sub>n</sub>] and poly(β-benzyl L-aspartate,[1-<sup>13</sup>C]glycine) [(Asp(OBzl),Gly\*)<sub>n</sub>]. [1-<sup>13</sup>C]Gly NCA content of about 5% was chosen for the preparation of (Ala,Gly\*)<sub>n</sub> and about 8% for the other copolypeptides. For all these samples, the value of the A/I ratio was 100. The α-helical form of (Asp(OBzl),Gly\*)<sub>n</sub> was converted to the ω-helical form by heating at 123 °C for 10 min. Synthetic conditions and characterization of the samples used here are summarized in Table I.

**<sup>13</sup>C NMR Measurement.** <sup>13</sup>C CP-MAS NMR spectra were recorded at 67.80 MHz with a JEOL GX-270 spectrometer equipped with a CP-MAS accessory at room temperature. Field strength of the <sup>1</sup>H decoupling was 12 mT. A contact time was 2 ms, and repetition time was 5 s. Spectral width and data points were 40 kHz and 8K, respectively. Samples were placed in a bullet-type rotor and spun as fast as 3–4 kHz. Powder pattern spectra were recorded with the same instrument without magic angle spinning. Spectra were usually accumulated 100–2000 times to achieve a reasonable signal-to-noise ratio. <sup>13</sup>C chemical shifts were calibrated indirectly through external benzene (128.5 ppm relative to tetramethylsilane ((CH<sub>3</sub>)<sub>4</sub>Si)).

To obtain the three principal components of shielding tensors<sup>30</sup> (σ<sub>11</sub>,

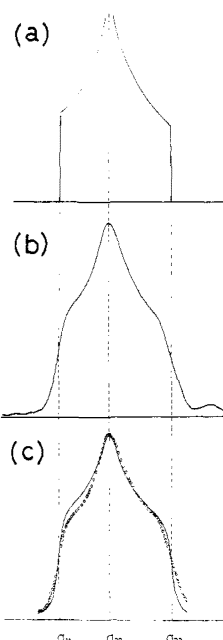


**Figure 1.** Schematic representations of (a) theoretical powder pattern, (b) experimental powder pattern, and (c) theoretical powder pattern convoluted with the Lorentzian function (circles are experimental points) for (Gly\*)<sub>n</sub> I.

σ<sub>22</sub>, and σ<sub>33</sub>, from the downfield to upfield), we fitted the theoretical powder pattern line shape which is convoluted with Lorentzian function (symmetrical broadening function) to the observed powder patterns as shown in Figure 1, where the line-shape function *I*(σ) is expressed by Bloembergen and Rowland<sup>16</sup>

$$I(\sigma) \propto \frac{K(m)}{(\sigma_{33} - \sigma)(\sigma_{22} - \sigma_{11})} \quad (1)$$

where

$$m = \frac{(\sigma - \sigma_{11})(\sigma_{33} - \sigma_{22})}{(\sigma_{33} - \sigma)(\sigma_{22} - \sigma_{11})} \quad \text{for } \sigma_{11} \leq \sigma < \sigma_{22}$$

and

$$I(\sigma) \propto \frac{K(m)}{(\sigma - \sigma_{11})(\sigma_{33} - \sigma_{22})} \quad (2)$$

where

$$m = \frac{(\sigma_{33} - \sigma)(\sigma_{22} - \sigma_{11})}{(\sigma - \sigma_{11})(\sigma_{33} - \sigma_{22})} \quad \text{for } \sigma_{22} < \sigma \leq \sigma_{33}$$

in which *K*(*m*) is the complete elliptic integral of the first kind as given by

$$K(m) = \int_0^{\pi/2} (1 - m^2 \sin^2 \phi)^{1/2} d\phi \quad (3)$$

(30) The value of σ<sub>22</sub> can be read exactly from the observed powder pattern spectra. For this, the error limit of σ<sub>22</sub> is smaller than ±1 ppm. However, the error limit of σ<sub>11</sub> and σ<sub>33</sub> is much larger than that of σ<sub>22</sub>. Therefore, the error limit of the fitting for the observed powder pattern spectra would be ±1 ppm, unless otherwise specified.

- (15) Astbury, W. T. *Nature (London)* **1949**, *163*, 722.
- (16) Bloembergen, N.; Rowland, J. A. *Acta Metallurg.* **1953**, *1*, 731.
- (17) Saitō, H.; Iwanaga, Y.; Tabeta, R.; Narita, M.; Asakura, T. *Chem. Lett.* **1983**, 427.
- (18) Avignon, M.; Garrigou-Lagrange, C. *Spectrochim. Acta* **1971**, *27A*, 297.
- (19) Borona, G. N.; Toniolo, C. *Gazz. Chim. It.* **1980**, *110*, 503.
- (20) Toniolo, C.; Borona, G. M.; Rajasekharan Pillai, V. N.; Mutter, M. *Macromolecules* **1980**, *13*, 772.
- (21) Johnson, C. E.; Bovey, F. A. *J. Chem. Phys.* **1958**, *29*, 1012.
- (22) Toniolo, C. *Macromolecules* **1978**, *11*, 437.
- (23) Lifson, S.; Sander, C. *Nature (London)* **1979**, *282*, 109.
- (24) Kubota, S.; Fasman, G. D. *Biopolymers* **1975**, *14*, 605.
- (25) Yamashita, O.; Yamane, T.; Ashida, T.; Yamashita, S.; Yamashita, T. *Polym. J.* **1979**, *11*, 763.
- (26) In parallel to this work, we are studying some polymer (polyoxymethylene) structures by solid-state NMR, and we have observed the difference in the tensor components between its crystalline and amorphous structure regions, of which the isotropic chemical shifts are identical. However, polypeptides generally do not take the amorphous state in the crystalline sample.
- (27) Lotz, B. *J. Mol. Biol.* **1974**, *87*, 169.
- (28) Ramachandran, G. N.; Sasisekharan, V.; Ramakrishnan, C. *Biochim. Biophys. Acta* **1966**, *112*, 168.
- (29) McGuire, R. F.; Vanderkooi, G.; Momany, F. A.; Ingwall, T. T.; Crippen, G. M.; Lotan, N.; Tuttle, R. W.; Kashuba, K. L.; Scheraga, A. *Macromolecules* **1971**, *4*, 112.

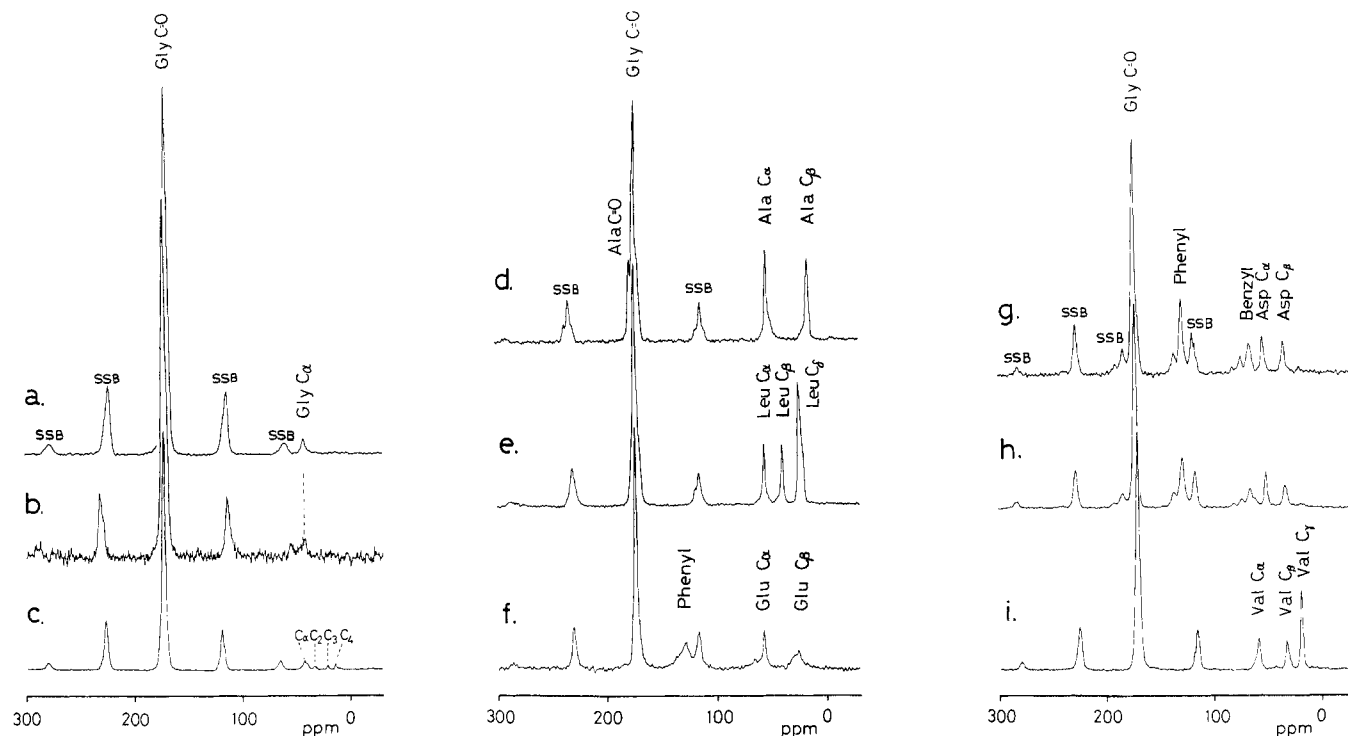


**Figure 2.**  $^{13}\text{C}$  CP-MAS NMR spectra (68.50 MHz) of poly( $[1-^{13}\text{C}]$ glycine) and  $[1-^{13}\text{C}]$ glycine-containing polypeptides. (a)  $(\text{Gly}^*)_n$  I, (b)  $(\text{Gly}^*)_n$  II, (c)  $(\text{Gly}^*)_5$ , (d)  $(\text{Ala,Gly}^*)_n$ , (e)  $(\text{Leu,Gly}^*)_n$ , (f)  $(\text{Glu(OBzl),Gly}^*)_n$ , (g)  $(\text{Asp(OBzl),Gly}^*)_n$  ( $\alpha$ -helix), (h)  $(\text{Asp(OBzl),Gly}^*)_n$  ( $\omega$ -helix), (i)  $(\text{Val,Gly}^*)_n$ .

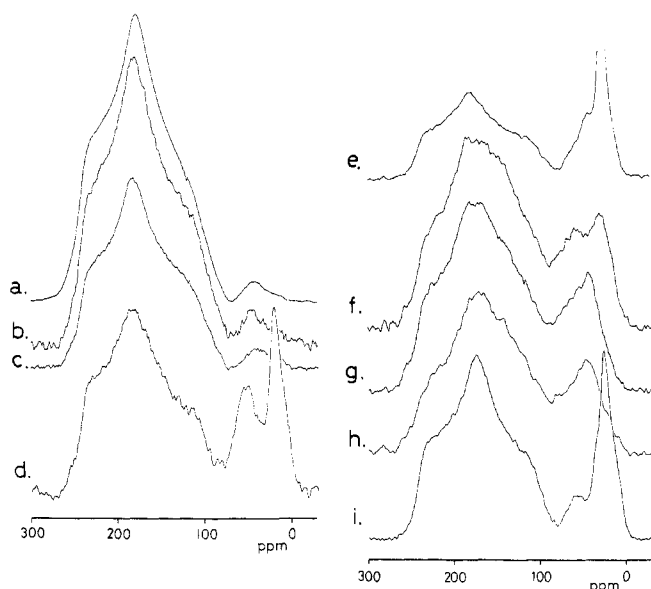


**Figure 3.**  $^{13}\text{C}$  NMR (68.50 MHz) powder pattern spectra of poly( $[1-^{13}\text{C}]$ glycine) and  $[1-^{13}\text{C}]$ glycine-containing polypeptides. (a)  $(\text{Gly}^*)_n$  I, (b)  $(\text{Gly}^*)_n$  II, (c)  $(\text{Gly}^*)_5$ , (d)  $(\text{Ala,Gly}^*)_n$ , (e)  $(\text{Leu,Gly}^*)_n$ , (f)  $(\text{Glu(OBzl),Gly}^*)_n$ , (g)  $(\text{Asp(OBzl),Gly}^*)_n$  ( $\alpha$ -helix), (h)  $(\text{Asp(OBzl),Gly}^*)_n$  ( $\omega$ -helix), (i)  $(\text{Val,Gly}^*)_n$ .

The  $\sigma_{33}$  component is sometimes overlapped with other peaks such as the methylene, phenyl, or ester carbons. Thus, we determined this component by using the value of the isotropic chemical shift by the CP-MAS experiment and the remaining two components.<sup>31</sup>

(31) In principle, the isotropic CO signal could be split into an asymmetric doublet due to the presence of  $^{14}\text{N}$ - $^{13}\text{C}$  dipolar interaction (ref 32). This contribution, however, turned out to be very small when the  $^{13}\text{C}$  NMR spectra are recorded at higher magnetic field ( $\geq 7$  T) (ref 33). In fact, we found that symmetric single signals were obtained for the present case, as shown in Figure 2. Therefore, we completely neglected this contribution for our data analysis of powder pattern spectra.

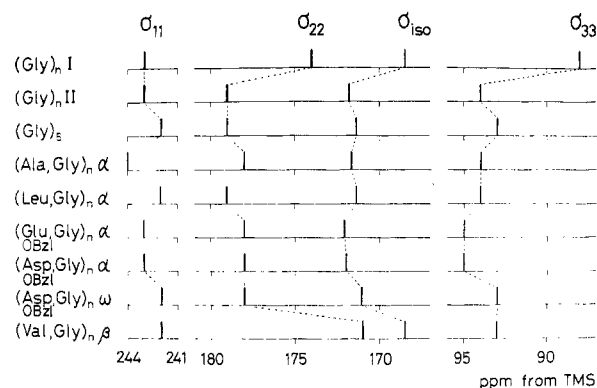


**Figure 4.** Observed stick spectra of  $^{13}\text{C}$  NMR isotropic chemical shifts and tensor components of glycine carbonyl carbons of poly( $[1-^{13}\text{C}]$ glycine) and  $[1-^{13}\text{C}]$ glycine-containing polypeptides.

## Results and Discussion

**Poly( $[1-^{13}\text{C}]$ glycine).** Figure 2a-c and Figure 3a-c show 67.80-MHz  $^{13}\text{C}$  CP-MAS NMR spectra and powder pattern spectra, respectively, of  $(\text{Gly})_n$  I,  $(\text{Gly})_n$  II, and  $(\text{Gly})_5$ . All the isotropic chemical shifts and tensor components determined from these spectra are tabulated in Tables II and III and Figure 4. The CO chemical shift of  $(\text{Gly})_n$  II is displaced downfield by 3.3 ppm with respect to that of  $(\text{Gly})_n$  I, although the  $\text{C}_\alpha$  chemical shifts of both forms are resonated at the same position. The value of 3.3 ppm is slightly different from that reported previously<sup>6,17</sup> (3.9 ppm), but they are within allowable experimental error. Closer examination of the tensor components exhibits a significant difference of 4~5 ppm for  $\sigma_{22}$  and  $\sigma_{33}$  in going from  $(\text{Gly})_n$  I to  $(\text{Gly})_n$  II, and it is larger compared with the case of the isotropic chemical shift, whereas  $\sigma_{11}$  is generally insensitive to conformational change as mentioned later. The breadth of the chemical shift anisotropy ( $\sigma_{11} - \sigma_{33}$ ) of the form I is significantly larger than that of the form II.

In the  $^{13}\text{C}$  CP-MAS NMR spectrum of  $(\text{Gly})_5$ ,  $^{13}\text{C}$  signals from the terminal *n*-butylamide groups are easily discriminated and assigned straightforwardly in the same manner as the previous paper.<sup>2</sup> The  $\text{C}_1$  signal of its group is obscured by overlapping with

**Table II.**  $^{13}\text{C}$  Chemical Shifts of Polypeptides Containing Glycine Residues Characteristic of  $3_1$ -Helix,  $\alpha$ -Helix,  $\beta$ -Sheet, and  $\omega$ -Helix Forms ( $\pm 0.2$  ppm from TMS)

sample <sup>a</sup>	conformation <sup>b</sup>	$^{13}\text{C}$ chemical shift					ref
		carbonyl <sup>c</sup>	$\text{C}_\alpha$	$\text{C}_\beta$	phenyl	benzyl	
(Gly*) <sub>n</sub>	$\beta$	168.5 <sup>+</sup>	43.2				this work
(Gly*) <sub>n</sub>	$3_1$	171.8 <sup>+</sup>	43.2				this work
(Gly*) <sub>5</sub>		171.4 <sup>+</sup>	41.7				this work
(Gly) <sub>n</sub>	$\beta$	168.4	43.2				17
		169.2	44.3				8
(Gly) <sub>n</sub>	$3_1$	172.3	43.2				6
		172.1	42.0				8
(Ala,Gly*) <sub>n</sub>	$\alpha$	176.7	52.2	14.6			this work
		171.7 <sup>+</sup>					
(Ala) <sub>n</sub>	$\alpha$	176.4	52.4	14.9			2
		176.8	52.8	15.5			8
	$\beta$	171.8	48.2	19.9			2
		172.2	49.3	20.3			8
(Leu,Gly*) <sub>n</sub>	$\alpha$	171.4 <sup>+</sup>	55.4	39.0			this work
(Leu) <sub>n</sub>	$\alpha$	175.7	55.7	39.5			1
	$\beta$	170.5	50.5	43.3			1
(Glu(OBzl),Gly*) <sub>n</sub>	$\alpha$	172.1 <sup>+</sup>	56.5	25.3	127.5	65.2	this work
(Glu(OBzl)) <sub>n</sub>	$\alpha$	175.6	56.4	25.6	~128.5	66.0	5
		175.4	56.8	25.9			8
	$\beta$	171.0	51.2	29.0			5
		172.2	51.1	29.7			8
(Asp(OBzl),Gly*) <sub>n</sub>	$\alpha$	172.0 <sup>+</sup>	53.2	33.8	127.8	65.9	this work
(Asp(OBzl),Gly*) <sub>n</sub>	$\omega$	171.1 <sup>+</sup>	50.8	33.2	127.7	65.3	this work
(Asp(OBzl)) <sub>n</sub>	$\alpha$	174.9	53.4	33.8	129.8	65.7	3
		174.9	53.6	34.2	128.2	66.1	8
	$\alpha_L$	171.1	50.9	33.8	129.2	66.1	3
	$\omega$	171.3	50.5	32.9	129.0	65.3	3
	$\beta$	169.6	49.2	35.1	129.2	65.9	3
(Val,Gly*) <sub>n</sub>	$\beta$	168.5 <sup>+</sup>	58.0	32.0			this work
(Val) <sub>n</sub>	$\alpha$	174.9	65.5	28.7			1
	$\beta$	171.8	58.4	32.4			1
		171.5	58.2	32.4			8

<sup>a</sup> Symbol \* indicates carbonyl carbon enriched by  $^{13}\text{C}$ . <sup>b</sup>  $\alpha$ -Helix is right-handed unless otherwise specified. <sup>c</sup> Symbol + indicates chemical shift of glycine residue.

**Table III.**  $^{13}\text{C}$  Chemical Shift Tensor Components of Glycine Carbonyl Carbons (ppm from TMS)

sample <sup>a</sup>	conformation	tensor component <sup>b</sup>			anisotropy breadth	
		$\sigma_{11}$	$\sigma_{22}$	$\sigma_{33}$	$\Delta\sigma^c$	$\sigma_{11} - \sigma_{33}$
(Gly*) <sub>n</sub> I	$\beta$	243	174	88	-121	155
(Gly*) <sub>n</sub> II	$3_1$	343	179	94	-117	149
(Gly*) <sub>5</sub>		242	179	93	-118	149
(Ala,Gly*) <sub>n</sub>	$\alpha$	244	178	94	-116	150
(Leu,Gly*) <sub>n</sub>	$\alpha$	242	179	94	-117	148
(Glu(OBzl),Gly*) <sub>n</sub>	$\alpha$	243	178	95 <sup>d</sup>	-116	148
(Asp(OBzl),Gly*) <sub>n</sub>	$\alpha$	243	178	95 <sup>d</sup>	-116	148
(Glu(OBzl),Gly*) <sub>n</sub>	$\omega$	242	178	93 <sup>d</sup>	-117	149
(Val,Gly*) <sub>n</sub>	$\beta$	242	171	93	-114	149

<sup>a</sup> Symbol \* indicates carbonyl carbon enriched by  $^{13}\text{C}$ . <sup>b</sup> Uncertainty  $\pm 1$  ppm, unless otherwise specified. <sup>c</sup>  $\Delta\sigma = \sigma_{33} - 1/2(\sigma_{11} + \sigma_{22})$ . <sup>d</sup> The line shape of glycine residue is obscure and the value of the tensor component  $\sigma_{33}$  is tentative (uncertainty  $\pm 2 \sim 3$  ppm) because of the overlap with the  $\text{C}_\alpha$  signal of the host residue.

the  $\text{C}_\alpha$  carbon, which is resonated at 41.7 ppm. The Gly  $\text{C}_\alpha$  signal in (Gly)<sub>n</sub> of higher molecular weight is found to be generally insensitive to the conformational change but the  $\text{C}_\alpha$  signal of (Gly)<sub>5</sub> displaced upfield by 1.5 ppm relative to (Gly)<sub>n</sub>, and it may be regarded as a significant change. But, the CO signal of (Gly)<sub>5</sub> is resonated in the vicinity of that of (Gly)<sub>n</sub> II. All the tensor components of (Gly)<sub>5</sub> are not far from those of (Gly)<sub>n</sub> II and are apparently distinct from those of (Gly)<sub>n</sub> I. In addition, it was reported that Ac(Gly)<sub>n</sub>NHET (n = 1-4)<sup>18</sup> takes the ternary helix conformation like (Gly)<sub>n</sub> II, and *t*-Boc(Gly)<sub>3</sub>OMe<sup>19,20</sup> exhibits the IR absorption bands not far from the frequencies as expected for (Gly)<sub>n</sub> II. IR absorption bands on (Gly)<sub>5</sub> are close to these reported ones. These facts indicate that this sample takes a structure close to (Gly)<sub>n</sub> II, and this view is also supported by our IR experiment.

**Copolyptide.** Figure 2d-i shows  $^{13}\text{C}$  CP-MAS NMR spectra of so-called host polypeptides containing [ $^{13}\text{C}$ ]glycine residues. First, we consider  $^{13}\text{C}$  CP-MAS NMR spectra of (Ala,Gly\*)<sub>n</sub> containing 5% Gly residues. In addition to a sharp intense Gly CO peak, small peaks of Ala  $\text{C}_\alpha$ ,  $\text{C}_\beta$ , and CO were observed. A comparison of the  $^{13}\text{C}$  chemical shifts of these carbons with the reference data of (Ala)<sub>n</sub> reported previously leads to the fact that the (Ala,Gly\*)<sub>n</sub> samples take the  $\alpha_R$ -helix form. Thus, it is suggested that the Gly residue in the copolymer also takes the  $\alpha$ -helix form. The Gly CO carbon signal of 171.7 ppm ( $\alpha$ -helix) is resonated at the position close to (Gly)<sub>n</sub> II ( $3_1$ -helix), and this result coincides with that of Kricheldorf et al.<sup>7</sup> They reported that the signal of the  $\alpha$ -helix Gly CO absorbs ca. 3 ppm downfield of its  $\beta$ -sheet position.<sup>9</sup> Further, the powder pattern spectra (Figure 3b and d) are quite similar between the  $\alpha$ -helix and  $3_1$ -helix. Thus, it is difficult to differentiate the  $\alpha$ -helix from  $3_1$ -helix by displacement of the Gly  $^{13}\text{C}$  chemical shift alone.

Further, we consider  $^{13}\text{C}$  CP-MAS NMR spectra of the other  $\alpha$ -helical polypeptides. It is obvious that the other copolyptide samples take the  $\alpha$ -helix form, as viewed from the  $^{13}\text{C}$  chemical shifts of the "host" Leu, Asp(OBzl), and Glu(OBzl) residues.<sup>2,3,5</sup> The  $^{13}\text{C}$  chemical shift positions are very close to those of corresponding homopolymers as well as the samples of (Ala,Gly\*)<sub>n</sub>, except for the phenyl carbons of the (Asp(OBzl),Gly\*)<sub>n</sub> and (Glu(OBzl),Gly\*)<sub>n</sub> (Table II). This shows that there are no effects of the sequence on the isotropic  $^{13}\text{C}$  chemical shifts. Interestingly, the  $^{13}\text{C}$  NMR peaks of the phenyl carbons in (Asp(OBzl),Gly\*)<sub>n</sub> and (Glu(OBzl),Gly\*)<sub>n</sub> are resonated upfield by 1.3-2.0 ppm relative to the respective homopolypeptide. Such a large upfield shift caused by incorporation of the Gly residue may be explained by the ring current effect due to the stacking arrangement of the benzene rings<sup>21</sup> at the end of the side chains. However, the whole side-chain conformation of the host amino acids may not have been changed drastically, because the other signals of the side chain are not displaced with respect to the corresponding homopoly-

peptides. The CO chemical shift of the Gly residue in (Leu,Gly\*)<sub>n</sub> is resonated slightly upfield by 0.3 ppm relative to (Ala,Gly\*)<sub>n</sub>, whereas those of (Asp(OBzl),Gly\*)<sub>n</sub> and (Glu(OBzl),Gly\*)<sub>n</sub> are resonated downfield by 0.3–0.5 ppm relative to it. It is considered that this effect is ascribed to the magnetic anisotropy of carbonyl carbons on the ring current of the benzene rings in the side chains of the host polypeptides. For the powder pattern of (Asp(OBzl),Gly\*)<sub>n</sub> and (Glu(OBzl),Gly\*)<sub>n</sub>, the line shapes of the glycine residue are rather obscured, because there also exist carbonyl peaks in the same region and phenyl peaks of the Asp(OBzl) and Glu(OBzl) residues. Then, the values of the tensor component  $\sigma_{33}$  determined from the powder pattern spectra as tabulated in Table III<sup>34</sup> are tentative (uncertainty  $\pm 2 \sim 3$  ppm) because of the overlap with the C $_{\alpha}$  signal of the host residue.

Further, we have reported <sup>13</sup>C CP-MAS and powder pattern spectra of the (Asp(OBzl),Gly\*)<sub>n</sub> sample in the  $\omega$ -helix form converted from the  $\alpha$ -helix form. The C $_{\alpha}$ , C $_{\beta}$ , and benzyl signals of the sample are shifted upfield by 2.4, 0.6, and 0.6 ppm, respectively, relative to the  $\alpha$ -helix, which are in good agreement with our previous data of the homopolypeptide.<sup>3</sup> The Gly CO chemical shift is also displaced upfield by 0.8 ppm, and this difference can be used as a means of differentiating the  $\omega$ -helix conformation from the 3<sub>1</sub>-helix or  $\alpha$ -helix conformation. However, we cannot distinguish the  $\alpha$ -helical and  $\omega$ -helical structure on the basis of the powder pattern spectrum.

As shown in Table II, the CO chemical shift of the (Val,Gly\*)<sub>n</sub> sample is quite close to (Gly)<sub>n</sub> I, consistent with the presence of the  $\beta$ -sheet structure. However, the values of the tensor components of (Val,Gly\*)<sub>n</sub> are different from those of (Gly)<sub>n</sub> I. Obviously, the value of  $\sigma_{22}$  is significantly displaced upfield by 3 ppm relative to (Gly)<sub>n</sub> I, which can be exactly determined. It is reported that valine residue is particularly favored in the "parallel- $\beta$ " region of the proteins<sup>22,23</sup> and that poly(L-valine) does not take the same antiparallel- $\beta$ -pleated sheet as taken in (Gly)<sub>n</sub> I.<sup>24</sup> Yamashita et al. showed that a large contraction of the *c* axis (fiber axis) occurs in (Val)<sub>n</sub> and (Ile)<sub>n</sub> in the  $\beta$ -sheet (*c* = 6.59

and 6.6 Å, respectively) relative to that of the  $\beta$ -sheet (Ala)<sub>n</sub> (*c* = 6.89 Å).<sup>25</sup> Thus, such a difference in the  $\sigma_{22}$  value is caused by the changes of the  $\beta$ -sheet structure between them. It is likely that such tensor components may become a useful tool to distinguish between the distinct structures which have a same isotropic chemical shift.<sup>26</sup>

**Conformation-Dependent Change of the Principal Values.** As mentioned above, all of the most shielded component  $\sigma_{33}$  are within the allowable experimental error, and this component is quite insensitive to the conformational change of the skeletal bonds. From the recent work<sup>13</sup> on the solid-state <sup>13</sup>C NMR of the [1-<sup>13</sup>C]glycyl-[<sup>15</sup>N]glycine HCl H<sub>2</sub>O single crystal, the directions of the principal axes of the carbonyl chemical shift tensor of the glycine residue have been determined. The  $\sigma_{22}$  component lies approximately along the carbonyl bond, and the  $\sigma_{33}$  is perpendicular to the plane defined by the amide oxygen, carbon, and nitrogen. The  $\sigma_{11}$  component is perpendicular to both the direction of  $\sigma_{22}$  and  $\sigma_{33}$ . Then, it is considered from the tensor components determined above that the electronic structure along the direction of principal axis for  $\sigma_{22}$  and  $\sigma_{33}$  is more closely related to the local conformation.

The hydrogen bonding also takes an important role in determining chemical shift. In fact, the formation of hydrogen bonding causes a significant downfield displacement of the Gly CO signal in our study on the collagen-like copolypeptide.<sup>6</sup> Similarly, the strong hydrogen bond is formed in (Gly)<sub>n</sub> II and the  $\alpha$ -helical copolypeptide, while the NH...OC hydrogen bond length of (Gly)<sub>n</sub> I (2.95 Å)<sup>27</sup> is rather longer than that for form II (2.73 Å)<sup>14,28</sup> and deviates markedly from linearity. For the  $\omega$ -helical sample, it seems that the hydrogen bond is slightly weaker than form II and  $\alpha$ -helix, because the isolated  $\omega$ -helix polypeptide is reported to be less favorable compared to the isolated  $\alpha$ -helix polypeptide by McGuire et al.<sup>29</sup> It is interesting that the direction of the most sensitive component  $\sigma_{22}$  is the same as that of the CO bond. Therefore, such displacements of the Gly CO signals could be mainly accounted for by the manner of the hydrogen bonding.

For elucidating the contribution of hydrogen bonding to the chemical shift and that of conformational change, the quantum chemical calculation of <sup>13</sup>C shielding constants and tensors was ascertained to be very effective,<sup>10,11</sup> and such calculations on the glycine dipeptide model are under way.

Obviously, collection of the principal component of the chemical shift is more valuable to chemical structure than that of only isotropic <sup>13</sup>C chemical shifts, but in some instances, the inherent larger experimental errors of tensor components make determination of the exact principal elements difficult (the obscure powder pattern spectra, for example, (Asp(OBzl),Gly\*)<sub>n</sub>).

(32) Hexem, J. G.; Frey, M. H.; Opella, S. J. *J. Am. Chem. Soc.* **1981**, *103*, 224.

(33) Saitô, H.; Tabeta, R.; Shoji, A.; Ozaki, T.; Ando, I.; Asakura, T. "Magnetic Resonance in Biology and Medicine", Govil, G.; Khatri, C. L.; Saran, A., Eds.; Tata McGraw-Hill: New Delhi, 1985 p 195.

(34) It is apparent that natural abundant <sup>13</sup>C of non-glycyl residues gave about 10% of the entire carbonyl signal. For simplicity, we neglected contribution of this peak for the analysis of the powder pattern spectrum. In fact, the line shape of this sample agrees with that of another sample containing host residue [(Ala,Gly\*)<sub>n</sub> (<sup>13</sup>C-enriched glycine content 13%) natural abundant <sup>13</sup>C of host residue gives about 6%] within the experimental error (data not shown).